NURETH14-318

SENSITIVITY AND UNCERTAINTY ANALYSIS OF DEBRIS BED COOLABILITY

S. E. Yakush¹, P. Kudinov² and N. T. Lubchenko³

¹ A. Yu. Ishlinskii Institute for Problems in Mechanics of the Russian Academy of Sciences, Moscow, Russia

² Royal Institute of Technology (KTH), Stockholm, Sweden ³ Moscow Institute of Physics and Technology, Dolgoprudniy, Russia

Abstract

Theoretical studies of top-fed debris bed coolability available so far have been focused on obtaining the Dryout Heat Flux (DHF) as a function of debris bed parameters (mean particle diameter and porosity). In this paper, uncertainty analysis is carried out to quantify the influence of different factors on DHF. Global sensitivity analysis is applied to rank the drag model parameters according to their effects on DHF and average pressure drop (epistemic uncertainty). The most influential model parameters are then optimized to achieve the best fit to experimental data available. Finally, aleatory uncertainties due to randomness of the debris bed formation scenario and respective physical parameters (particle diameter, porosity) are quantified.

Introduction

Recent events at Fukushima Daichi plant reminded once again that severe accidents do occur in reality and reliable mitigation measures are extremely important for the minimization of accident consequences. Ex-vessel core melt stabilization strategy during a hypothetic severe accident in Swedish-type BWRs is based on the melt fragmentation in a deep pool of water and formation of a porous debris bed at the bottom of the reactor pit. Decay heat generated by the debris bed has to be removed by natural circulation to prevent the dryout and melting of the debris. Otherwise, decay heat accumulation in a non-coolable bed, remelting of the debris and melt attack on the concrete basemat presents a credible threat to the containment integrity.

The problem of the debris bed coolability has received substantial attention in the past. Of the recent and ongoing activities aimed at the in-depth study of coolability phenomena, the programs DEFOR, PEARL, QUENCH and DEBRIS currently performed in the framework of SARNET-2 project, are worth mentioning (see the current status in [1]).

The classical simplification used to obtain the critical coolability conditions was to consider a uniform flat debris bed in saturated water (top-fed debris bed), with counter-current flows of water (flowing down) and vapor (flowing up), or a bottom-fed debris bed with vertical water inflow through the bottom boundary. In the one-dimensional case, the critical conditions are conveniently expressed in terms of the Dryout Heat Flux (DHF), or the heat release rate per

unit area of debris bed top surface [2-7]. A number of experiments aimed at obtaining the relationship between the DHF and debris bed parameters, i.e., mean particle diameter, porosity, has been carried out [8-10]. In these experiments, either the pressure drop in the debris bed was obtained, or conditions at which dryout zones occur in the debris bed were measured directly and compared with the predictions of different models.

Since the two-phase flow in the debris bed is governed by drag and gravity, different values of DHF are obtained from different drag models. From the reactor safety point of view, it is important not only to obtain the conditions at which debris bed dryout can occur, but also to assess the uncertainties related to (i) intrinsic variability of debris bed properties (i.e., particle size and porosity), which generally depend on melt ejection conditions, and uncertainty in the system pressure, which depend on the plant accident scenario; and (ii) deficiencies and incompleteness of the models used (drag laws). In this paper, global sensitivity analysis based on the Morris diagrams and Sobol sensitivity indices is presented in order to rank the importance of different input and model parameters and to quantify the influence of physical factors on the uncertainty in prediction of dryout heat flux and pressure drop in top-fed and bottom-fed debris beds.

1. Problem Statement

1.1 Governing equations

The traditional scheme for the determination of dryout conditions in a flat debris bed is based on the one-dimensional approach. A steady-state solution is sought for the vertical distributions of void fraction α , superficial velocities j_i of liquid and gas phases (subscripts L and G, respectively), and pressure P, given the volumetric evaporation rate $\Gamma = Q/\Delta H_{ev}$, where Q is the heat release rate per unit volume of debris bed, ΔH_{ev} is the latent heat of evaporation. The phase continuity and momentum equations are

$$\rho_L \frac{dj_L}{dz} = -\Gamma, \quad \rho_G \frac{dj_G}{dz} = \Gamma \tag{1}$$

$$-\frac{dP}{dz} - \rho_L g = \frac{\mu_L}{KK_{rL}} j_L + \frac{\rho_L}{\eta \eta_{rL}} |j_L| j_L - \frac{F_i}{1 - \alpha}$$
(2)

$$-\frac{dP}{dz} - \rho_G g = \frac{\mu_G}{KK_{-G}} j_G + \frac{\rho_G}{\eta \eta_{-G}} |j_G| j_G + \frac{F_i}{\alpha}$$
(3)

The equations are written in the coordinate system originating at the bottom boundary of the debris bed, with the z-axis pointing vertically upwards. Here, g is the gravity acceleration, ρ_i and μ_i are the phase densities and viscosities (i = L, G). The right-hand sides of Eqs. (2), (3) contain the phase drag due to porous medium with linear and quadratic terms (with the absolute, K, η , and relative, K_{ri}, η_{ri} , permeabilities and passabilities), as well as the

interphase drag F_i due to relative motion of phases. Saturated conditions corresponding to some system pressure P_{sys} and temperature $T_{sys} = T_{sat}(P_{sys})$ are assumed. Commonly, fresh water is assumed as the coolant. The physical parameters of both phases (ρ_i, μ_i) are calculated from the tabular data on the saturation line at P_{sys} (the effects of pressure variation with height are neglected).

1.2 Drag models

The permeability K and passability η are related to the porosity ε and mean particle diameter d by [11]

$$K = \frac{\varepsilon^3 d^2}{150(1-\varepsilon)^2}, \quad \eta = \frac{\varepsilon^3 d}{1.75(1-\varepsilon)}$$
 (4)

The relative permeabilities K_{ri} and passabilities η_{ri} as functions of the void fraction α are described by the power-law relations [2-4]:

$$K_{rL} = (1 - \alpha)^{nL}, \quad \eta_{rL} = (1 - \alpha)^{mL}$$

$$K_{rG} = \alpha^{nG}, \quad \eta_{rG} = \alpha^{mG}$$
(5)

In the "classic" models [2-4], the interphase drag is neglected, the exponents in the relative permeabilities are nL = nG = 3, and those in the relative passabilities, mL and mG, range from 3 to 6.

Of the models which explicitly take into account the interphase drag, the one by Schulenberg and Müller [5] is considered here:

$$K_{rL} = (1 - \alpha)^{nL}, \quad \eta_{rL} = (1 - \alpha)^{mL}, \quad K_{rG} = \alpha^{nG}, \quad \eta_{rG} = \begin{cases} 0.1 \alpha^{mGL}, & \alpha \le \alpha_* \\ \alpha^{mGH}, & \alpha > \alpha_* \end{cases}$$
(6)

$$F_{i} = C_{SM} \left(1 - \alpha \right)^{nSM} \alpha \frac{\rho_{L} K}{\eta \sigma} g \left(\rho_{L} - \rho_{G} \right) \left| j_{r} \right| j_{r}, \quad C_{SM} = 350, \quad nSM = 7$$

$$(7)$$

where nL=3, mL=5, nG=3, mGL=4, mGH=6, the boundary between two regimes for the gas passability is $\alpha_* = 0.1^{1/(mGH-mGL)} = 0.1^{1/2} \approx 0.316$, σ is the coefficient of surface tension at the liquid-vapor interface, $j_r = j_G/\alpha - j_L/(1-\alpha)$ is the relative phase velocity.

1.3 Pressure drop and Dryout Heat Flux

Under the above assumptions (uniformly heated homogeneous debris bed), the continuity equations (1) have linear solutions for the superficial velocities as functions of height:

The 14th International Topical Meeting on Nuclear Reactor Thermalhydraulics, NURETH-14 Toronto, Ontario, Canada, September 25-30, 2011

$$j_L = j_{LB} - \frac{Q}{\rho_L \Delta H_{ev}} z, \quad j_G = \frac{Q}{\rho_G \Delta H_{ev}} z$$
 (8)

where j_{LB} is the superficial velocity of liquid on the bottom boundary of the debris bed (positive for a bottom-fed, and zero for a top-fed debris bed).

For a given volumetric heat release rate Q, by eliminating the pressure gradient from Eqs. (2), (3), a non-linear equation is obtained

$$\left(\rho_{L} - \rho_{G}\right)g = \left(\frac{\mu_{G}}{KK_{rG}}j_{G} + \frac{\rho_{G}}{\eta\eta_{rG}}|j_{G}|j_{G}\right) - \left(\frac{\mu_{L}}{KK_{rL}}j_{L} + \frac{\rho_{L}}{\eta\eta_{rL}}|j_{L}|j_{L}\right) + F_{i}\left(\frac{1}{\alpha} + \frac{1}{1-\alpha}\right)$$
(9)

from which, after substitution of superficial velocities (8), the local void fraction α at any height $0 \le z \le H$ can be obtained (H is the debris bed height). With α known, the local pressure gradient can then be evaluated from Eqs. (2) or (3). Another important quantity is the average pressure gradient

$$-\frac{\Delta P}{H} - \rho_L g = \frac{1}{H} \int_0^H \left(-\frac{dP}{dz} - \rho_L g \right) dz \tag{10}$$

where ΔP is the pressure drop between the bottom and top of the debris bed. The right-hand side of Eq. (10) can be evaluated by the numerical integration.

For a uniformly heated, thermally insulated from the bottom, homogeneous debris bed considered here, the heat flux through a horizontal cross-section at a height z is equal to Qz. The highest heat flux HF = QH is attained on the debris bed top boundary. In the steady-state case, this heat flux is related to the superficial velocities of vapor j_{GT} and liquid j_{LT} at the debris bed top via Eq. (8):

$$HF = QH = j_{GT} \rho_G \Delta H_{ev} = (j_{LB} - j_{LT}) \rho_L \Delta H_{ev}$$
(11)

The limiting conditions for water inflow occur on the top boundary of the debris bed, where the upward vapor flux and void fraction are the highest. Upon the substitution of superficial phase velocities from Eq. (11) into Eq. (9), a quadratic equation for HF follows, with the coefficients depending on α (e.g. [5]). For any void fraction on the interval $0 \le \alpha \le 1$, a single positive root HF(α) exists which gives the heat flux at which such a void fraction is attained on the debris bed top.

The function $HF(\alpha)$ has a single maximum on the interval $0 \le \alpha \le 1$ corresponding to the highest heat flux for which a steady-state solution to Eqs. (1)-(3) exists [5]. The absence of steady state for higher heat fluxes is interpreted as the occurrence of dryout, therefore, the maximum value of HF is referred to as the Dryout Heat Flux (DHF):

$$DHF = \max_{0 \le \alpha \le 1} (HF) \tag{12}$$

2. Problem Parameters

The dryout heat flux and pressure drop depend on the properties of porous medium and operating conditions. In application to reactor safety, these parameters are accident scenario-dependent: e.g., the system pressure depends on the availability and effectiveness of spray cooling, maintaining of steam condensation capacity of the pressure suppression pool, possible activation of filtered and non-filtered containment venting, etc. The particle size and morphology distributions (which together define the porosity of the bed) are affected by both the scenario of melt release and inherent uncertainties in fuel-coolant interaction phenomena (e.g. melt jet and droplet fragmentation, particle formation [12, 13] and agglomeration [14], etc.). As there is a significant dependence of these input parameters on stochastic features of accident scenarios, we treat them as *aleatory* uncertainties by defining respective probability density distributions.

On the other hand, the mathematical model (1)-(12) that predicts the dryout heat flux at given operating conditions and properties of the debris bed involves a number of constants. These constants were obtained from a limited number of experiments and often differ between different authors, even for the same functional form of closing relationships. In this work, we consider these model coefficients as epistemic uncertainty in knowledge about physical phenomena determining the dryout heat flux. Traditionally, the models of different authors are taken "as is" in terms of the constants involved, and then their predictions are compared to some experimental data to see which model is more adequate (e.g., [9, 10]). Here, an alternative approach is taken: the functional form of the closing relationships (5)-(7) is maintained, however, the parameters involved are considered as variable in certain ranges, rather than numerical constants. The main idea behind this is to clarify which model parameters are the most influential, and to see if such a "generic" model can be optimized against a large set of experimental data. For example, the constants in Schulenberg and Müller's model [5] were obtained using two sets of experimental data: first, the interphase drag constants $C_{SM} = 350$ and nSM = 7 were evaluated from the experiments with zero liquid flux, after which the exponents in the relative passabilities were derived from separate experiments with different phase flow rates, using the above constants for the interphase drag, i.e., the constants in (6), (7) are interdependent. However, the interphase drag data used in [5] are rather scattered, which warrants the current study of model sensitivity to these parameters and also attempts to find more optimal values that can provide a better agreement with experimental data.

The ranges of physical and model parameters relevant to assessment of debris bed coolability are summarized in Table 1, and the reasons for their choice are discussed below.

The *physical* parameters include the mean particle diameter d, debris bed porosity ε , and the system pressure P_{sys} (for saturated conditions). Experiments on fuel-coolant interaction show that particles formed upon fragmentation of high-temperature melt in water without steam explosion are of 0.2-20 mm size [15]. The particle size distribution functions obtained in different experiments have maximum corresponding to the particles with the diameters of the order of few millimeters. In the drag models (4)-(7), however, the diameter d is the effective *mean* particle diameter that provides the same friction in the bed as the mixture of the

particles with original size distribution. The variation range for the mean particle sizes observed *in different experiments* is substantially narrower than the range of actual particle diameter variation within each experiment. As a reference, note that the mean particle diameters in FARO experiments were between 2 and 4.5 mm (estimated from the distribution functions in [15]), while finer particles can be expected in the case of vapor explosion. In this work, the range for variation of mean *d* is assumed to be from 1 to 5 mm.

The porosity of the debris bed ε depends on the material, interaction conditions, particle morphology etc. For example, in [8] results of dryout heat flux experiments in artificially packed beds with porosities between 26 and 41% are reported, while in DEFOR experiments carried out in KTH on formation of debris bed in the process of melt-coolant interaction with corium simulant materials, porosities as high as 50-70% were obtained [12]. A typical value used in most coolability studies is $\varepsilon = 40\%$, therefore, a range from 35 to 50% is assumed here for the porosity. Note that the porosity depends on the particle size distribution, shape, the debris packing method, etc. (e.g. see [16]). Therefore, there is no unique and straightforward relationship between the mean particle diameter and porosity. For this reason, d and ε are considered here as independent (uncorrelated) input parameters.

The system pressure P_{sys} depends on the accident scenario, e.g., activation of containment venting and efficiency of spray and pressure suppression pool in condensing of generated vapor. Filtered containment venting systems are automatically activated (by rupture disks) in Swedish BWRs at pressures higher than 4-5 bars. Here, the probable range for the system pressure variation is taken to be 1-4 bar.

Table 1 Parameter ranges

| Parameter | Description | Range | | | |
|---------------|--|----------|--|--|--|
| | Physical parameters | | | | |
| P_{sys} | System pressure, bar | 1-4 | | | |
| d | Mean particle diameter, mm | 1-5 | | | |
| ε | Porosity, [-] | 0.35-0.5 | | | |
| | Model parameters | | | | |
| nL | Exponent in relative permeability K_{rL} | 2-4 | | | |
| mL | Exponent in relative passability η_{rL} | 3-7 | | | |
| nG | Exponent in relative permeability K_{rG} | 2-4 | | | |
| mG | Exponent in relative passability η_{rG} | 3-7 | | | |
| C_{SM} | Constant in interphase drag for model [5] | 200-500 | | | |
| nSM | Exponent in the drag force in model [5] | 6-9 | | | |
| mGL | Exponent in η_{rG} for low void in model [5] | 3-4 | | | |
| mGH | Exponent in η_{rG} for high void in model [5] | 4-7 | | | |

The *model* parameters include the exponents in the relative phase permeabilities and passabilities (nL, nG, mL, mG), while Schulenberg and Müller's model with interphase drag also involves constants C_{SM} , nSM, mGL, and mGH. The uncertainty ranges for these parameters were chosen around the values in the original models. Note that all "classic" models [2-4] are described by a single equation (5), they differ only in the relative passability exponents, which are assumed to be equal: mL = mG. Also, the debris bed height H is not an independent parameter, as it enters Eqs. (1)-(12) only multiplied by Q, which gives the heat flux HF at the top of debris bed (see Eq. (11)). This flux can also be conveniently expressed through Eq. (11) in terms of the gas superficial velocity at the top of the debris bed $j_{GT} = QH / \rho_G \Delta H_{ev} = HF / \rho_G \Delta H_{ev}$.

3. Numerical implementation

To facilitate the sensitivity analysis and uncertainty studies, a FORTRAN90 code Cool1D was developed which calculates from Eqs. (1)-(10) either the value of DHF, or the pressure drop (local and average), together with other flow parameters (e.g., superficial phase velocities and void fraction at a given point). The input data for Cool1D includes the physical properties of debris bed (porosity ε , mean particle diameter d), operating conditions (system pressure P_{sys}), as well as the parameters of drag models (4)-(7), e.g., the exponents in the relative permeabilities and passabilities, nL, mL, nG, mG, mGL, and mGH, as well as the coefficients of the interphase drag model nSM and C_{SM} .

Sensitivity and uncertainty analysis was performed by running Cool1D coupled with DAKOTA, Version 5.0 package [12]. The "black box" interaction model was used, in which DAKOTA was responsible for automatic generation of samples of input data corresponding to prescribed ranges and distribution functions, while Cool1D was called to perform calculations for each sample. The values of target functions (DHF or pressure drop) were fed back into DAKOTA for statistical analysis. To enable communication between the programs, appropriate interface scripts were developed.

4. Sensitivity analysis

4.1 Approach

When applying a model to the determination of dryout conditions, it is important to get a grasp on what parameters have the most pronounced influence on the dryout heat flux, and how important are interactions between different parameters. Screening sensitivity analysis was carried out by the Morris method [18] (see also [17, 19]) that allows one to determine factors which have (a) negligible, (b) linear and additive, or (c) non-linear factors or involved in interactions with other factors. The experimental plan proposed by Morris is composed of individually randomized 'one factor-at-a-time' (OAT) experiments. First, the range of variation of each input variable is mapped onto the interval [0, 1] and uniformly partitioned into p levels, creating a grid of p^k points at which evaluations of the model function $y(\mathbf{x})$ (DHF or pressure drop in our case) might take place, where k is the size of input vector \mathbf{x} . Then, r samples are generated randomly, and for a j-th input vector $\mathbf{x}^{(j)}$ the elementary effect

of the i-th input is computed by a forward or backward difference (chosen for the second point to remain on the interval [0, 1]):

$$d_i^{(j)} = \frac{y(\mathbf{x}^{(j)} + \Delta \mathbf{e}_i) - y(\mathbf{x}^{(j)})}{\Lambda}$$
(13)

where \mathbf{e}_i is *i*-th coordinate vector in the input space, $\Delta = p/2(p-1)$. Note that Δ is large (about half the input range), and Eq. (13) is not intended to approximate the local partial derivative, but to assess the variation of the model function with respect to the input vector in the whole domain. After generating r samples, the mean μ_i , modified mean μ_i^* and standard deviation σ_i are obtained for each input i:

$$\mu_{i} = \frac{1}{r} \sum_{i=1}^{r} d_{i}^{(j)}, \quad \mu_{i}^{*} = \frac{1}{r} \sum_{i=1}^{r} \left| d_{i}^{(j)} \right|, \quad \sigma_{i} = \sqrt{\frac{1}{r} \sum_{i=1}^{r} \left(d_{i}^{(j)} - \mu_{i} \right)^{2}}$$
(14)

The mean and modified mean give an indication of overall effect of an input on the output, whereas the standard deviation indicates the non-linear and interaction effects (because it shows the variation of input effect throughout the input space). Note that no assumptions are made on the distributions of the input parameters in the ranges presented in Table 1.

In the calculations presented hereafter, the number of levels was p=12, and the number of sample points r=500. Importantly, the reduction of number of levels to p=6 caused the variation in the μ_i^* and σ_i within 10%, while with the further reduction of the number of sample points to r=16, the difference in μ_i^* and σ_i with respect to the baseline values was within 20%. However, the qualitative view of the Morris diagrams, and all conclusions derived from them remained intact. This confirms that Morris method can be a very efficient tool for the screening analysis [19].

4.2 Results

4.2.1 Sensitivity of Dryout Heat Flux

In Fig. 1, the Morris diagrams are presented for DHF in a top-fed debris bed for the model and physical parameters listed in Table 1. Results are shown for the "classic" model (a) and Schulenberg and Müller's model (b), the model parameters are plotted by black and white points, the physical parameters are given in color. One can see that the most influential (i.e., having the largest value of μ^*) model parameters are the exponents in the relative phase passabilities mL and mG (mGH for model [5]). This means that, in the conditions close to dryout, the flowrates are high and the quadratic (passability-related) terms are the main contributors to the total drag. The superficial velocities of liquid are low due to high density ρ_L - see Eq. (8), and the influence of linear terms in the drag law (i.e., μ^* of parameter nL) is comparable with that of quadratic terms (parameter mL); for the gas the influence of parameter nG is negligible.

To elucidate this, consider the ratio of quadratic to linear drag forces for *i*-th phase at DHF which can be evaluated from Eqs. (2), (3), and (11), with Reed's model implied:

$$\xi_{i} = \frac{\rho_{i} \left| j_{i} \right| j_{i}}{\eta \eta_{ri}} \cdot \frac{KK_{ri}}{\mu_{i} j_{i}} = \frac{K}{\eta} \frac{\rho_{i}}{\mu_{i}} \frac{K_{rl}}{\eta_{rl}} \left| j_{i} \right| = \frac{1.75d}{150(1-\varepsilon)} \frac{\text{DHF}}{\alpha_{i}^{2} \mu_{i} \Delta H_{ev}}$$
(15)

For the smallest particles considered (d=1 mm, DHF=0.29 MW/m², $\alpha=0.75$) we obtain for the liquid phase $\xi_L=0.142$, for the gas phase $\xi_G=0.355$. For 3 mm particles (DHF=0.9 MW/m², $\alpha=0.769$) the ratios are $\xi_L=1.54$ and $\xi_G=3.21$, while for 5 mm particles (DHF=1.27 MW/m², $\alpha=0.771$) the ratios are $\xi_L=3.70$ and $\xi_G=7.48$. This means that quadratic drag terms are prevailing over the linear ones for particles with size over approximately 2 mm.

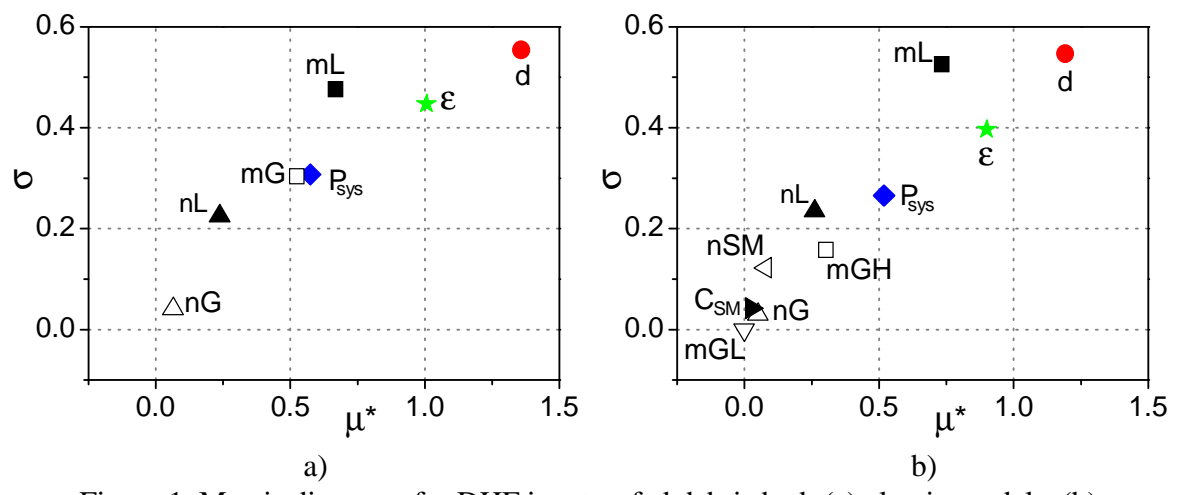


Figure 1 Morris diagrams for DHF in a top-fed debris bed: (a) classic models, (b) Schulenberg and Müller's model.

Importantly, the effects of the influential model parameters are comparable with those of the physical parameters, i.e., d, ε , and P_{sys} . The least influential are the coefficient C_{SM} and the exponent nSM in the interphase drag (7). Note that all points have significant coefficient of variance σ/μ^* . Therefore, nonlinearities and interactions between different factors are important, and none of the factors is additive.

Consider now the sensitivity of DHF to the model and physical parameters in the case of a bottom-fed debris bed. Calculations were carried out for two superficial velocities of liquid at the bottom boundary of the debris bed, $j_{LB} = 0.5$, 1, and 2 mm/s. In Figs. 2a-c the Morris diagrams are shown for Schulenberg and Müller's model. One can see that, with the increase in the flowrate, the influence on the DHF of all parameters, except P_{sys} , decreases significantly. This occurs because the dryout heat flux tends to the asymptotic value DHF = $j_{LB}\rho_L\Delta H_{ev}$ which has the physical meaning that the entering water must evaporate completely upon reaching the top boundary of the debris bed – see Fig. 2d, where the DHFs obtained from Reed's [3] (mL = mG = 5) and Schulenberg and Müller's [5] models are plotted

against j_{LB} for different particle diameters d. The influence of system pressure remains more noticeable, mainly through the density of the incoming fluid ρ_L .

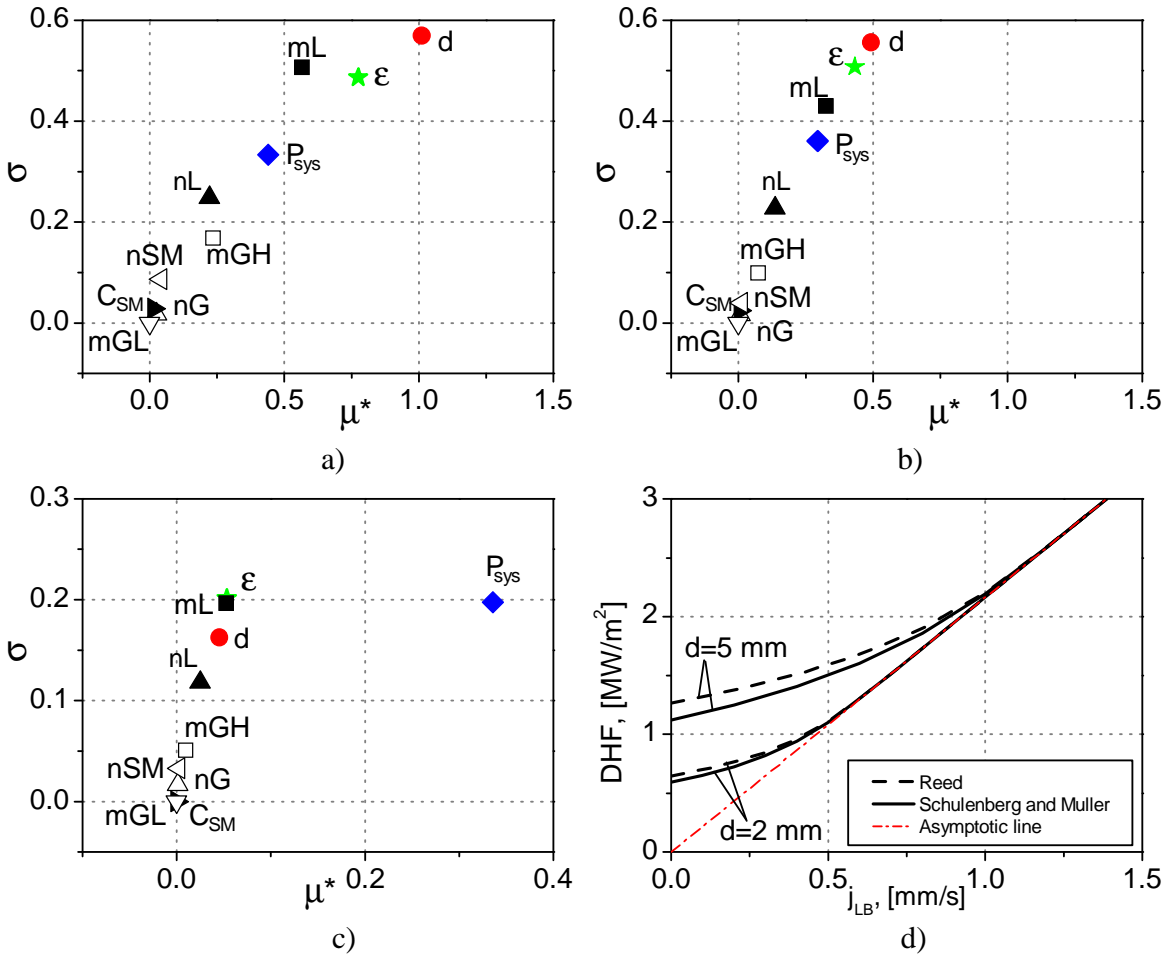


Figure 2 DHF in a bottom-fed debris bed: Morris diagrams for inflow superficial velocity $j_{LB} = 0.5 \text{ mm/s}$ (a), $j_{LB} = 1 \text{ mm/s}$ (b), $j_{LB} = 2 \text{ mm/s}$ (c) (Schulenberg and Müller's model); theoretical dependence of DHF on inflow velocity j_{LB} for $\varepsilon = 40\%$ and $P_{sys} = 1 \text{ bar}$ (d).

4.2.2 Sensitivity of pressure drop

The above results show that the influence of interphase drag model parameters on DHF is rather weak, both for the top-fed and bottom-fed debris beds. This can be explained by the high void fractions developing at the debris bed top at heat fluxes close to DHF. However, the pressure drop between the top and bottom of the debris bed (see Eq. (10)) is a quantity which is known to be much more sensitive to the interphase drag. It has been shown previously [7, 9, 10] that the "classical" models do not describe adequately the pressure drop in counter-current flow conditions. Therefore, in the current paper the sensitivity studies were focused on Schulenberg and Müller's model [5] which explicitly takes into account the interphase drag. Bottom-fed debris beds with the fixed inflow velocity j_{LB} at the bottom boundary and heat

flux (HF) removed through the top of the bed by coolant (or integral heat flux generated in the bed per unit area of the bed top surface) were considered. The target function was the average pressure drop, $-\Delta P/H - \rho_L g$ (see Eq. (10)).

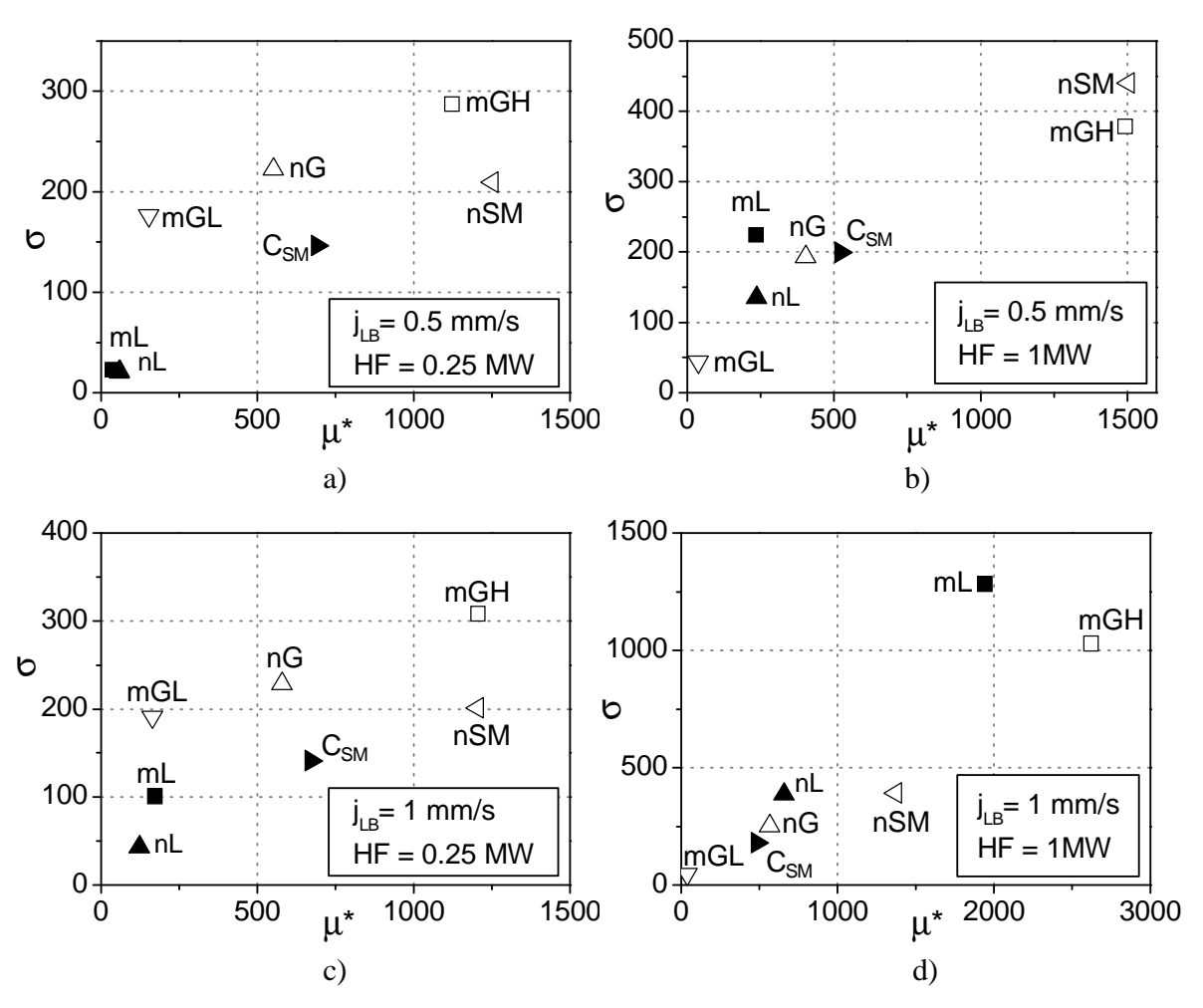


Figure 3 Morris diagrams for pressure drop in a bottom-fed debris bed (model [5]): (a) $j_{LB} = 0.5 \text{ mm/s}$, HF = 0.25 MJ/m² (gas superficial velocity and void fraction at debris bed top $j_{GT} = 0.18 \text{ m/s}$, $\alpha_T = 0.539$), (b) $j_{LB} = 0.5 \text{ mm/s}$, HF = 1 MJ/m² ($j_{GT} = 0.72 \text{ m/s}$, $\alpha_T = 0.788$), (c) $j_{LB} = 1 \text{ mm/s}$, HF = 0.25 MJ/m² ($j_{GT} = 0.18 \text{ m/s}$, $\alpha_T = 0.536$), (d) $j_{LB} = 3 \text{ mm/s}$, HF = 1 MJ/m² ($j_{GT} = 0.72 \text{ m/s}$, $\alpha_T = 0.756$).

The complete sensitivity analysis of pressure drop with respect to all physical and model parameters in the whole ranges presented in Table 1 (similar to that performed for DHF in Section 4.2.1) was not possible because for some input parameter combinations (samples generated by DAKOTA) the dryout heat flux DHF fell below the specified heat flux HF, and no steady-state solution could be found. Therefore, such analysis could be performed only for very low heat fluxes, which would be of limited practical value.

An alternative approach was taken in the current work: the analysis was carried out with the physical parameters fixed at d=3 mm, $\varepsilon=40\%$, and $P_{sys}=1$ bar, and the model parameters varying in the ranges given in Table 1. Two superficial velocities of liquid, $j_{LB}=0.5$ and 1 mm/s, were considered, and the heat flux at the debris bed top also took two values, 0.25 and 1 MW/m², which is below the DHF for both inflow velocities (1.23 and 2.17 MW/m² respectively).

In Fig. 3, the Morris diagrams for pressure drop sensitivity are presented for the four cases combining the above inflow velocity and heat flux values. The relative importance of interphase drag parameters varies with the conditions. E.g., the exponent *nSM* in the drag force is an influential parameter for low heating powers and inflow velocity (Figs. 3a-c), whereas in the conditions of high inflow and power (Fig. 3d), the predominant role is played by the porous drag parameters (the exponents in relative passabilities).

5. Model optimization

Sensitivity studies enabled ranking the model parameters with respect to their influence on DHF and pressure drop. The least influential parameters can be fixed at some values, while the most influential ones can be optimized against the relevant experimental data.

For the "classic" model (5), the exponents for relative permeabilities were fixed at the generally accepted values nL = nG = 3 [2-7], while an attempt was undertaken to find the optimum values for relative passability exponents mL and mG which would provide the best fit to the experimental data on DHF as a function of particle diameter (Fig. 4a). The experimental points in Fig. 4a in the range of particle diameters from 1 to 10 mm are taken from [7], where complete references to the original experimental works can be found. The target function for which the minimum value was sought was the standard deviation σ :

$$\sigma = V^{1/2}, \qquad V = \frac{1}{N_{\text{curp}}} \sum_{i=1}^{N_{\text{exp}}} (F_i - F_{i,\text{exp}})^2$$
 (16)

where V is the variance, $N_{\rm exp}$ is the number of experimental points, F_i and $F_{i,\rm exp}$ are the calculated and experimental values at i-th point. It turned out, however, that the optimization problem is ill-posed, since the response function does not possess a single well-defined minimum. Rather, a "valley" shown in Fig. 4b is observed on the (mL, mG) plane. This could be interpreted as the same DHF can be achieved by increasing the porous drag by one or another phase. A check was made to see if a minimum point exists, but is obscured by the scatter in the experimental data. However, even with an artificially generated DHF curve calculated from the original model by Reed [3], no distinct minimum was observed, albeit the "valley" became narrower. Additional data is necessary to find out the optimum values of the two parameters. Here, in line with all "classic" models, it was assumed that the exponents for both phases are equal. In this case, the optimum value can be easily found along the diagonal of the graph in Fig. 4b. The optimum values which give the best fit to all DHF data for a top-fed debris bed are mL = mG = 4.53, which is less than (but quite close to) the value 5 in Reed's drag model.

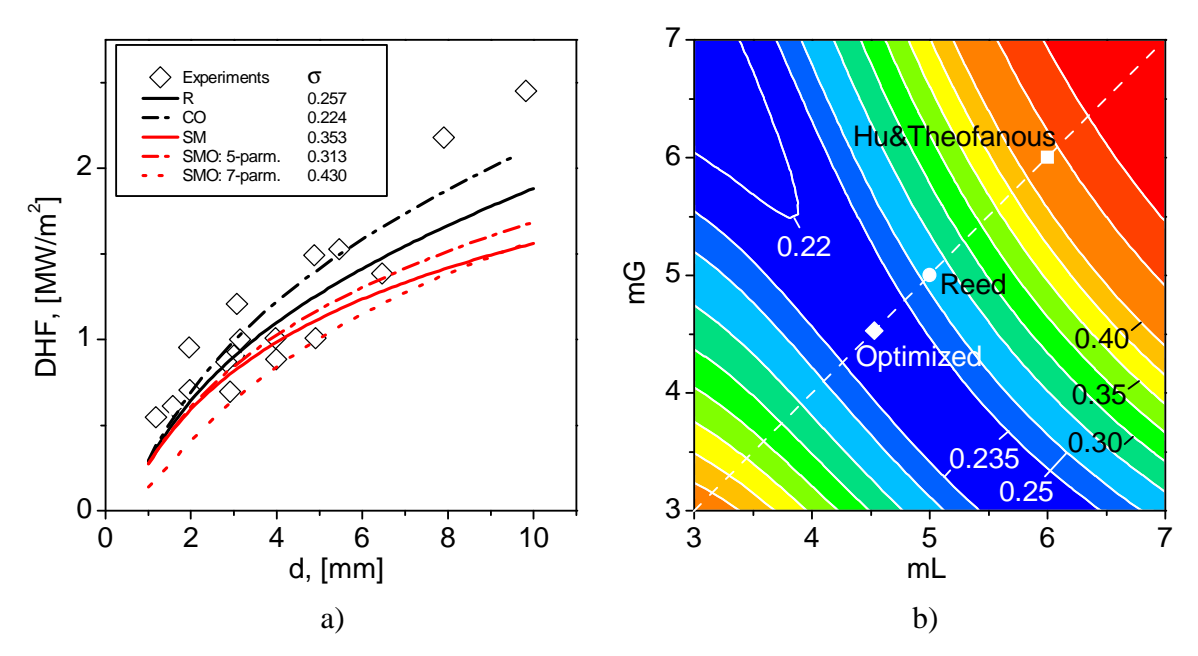


Figure 4 Optimization of models on DHF for top-fed debris bed: (a) comparison with experimental data summarized in [7]; (b) map of the standard deviation σ on the (mL, mG) plane.

Optimization of Schulenberg and Müller's model [5] was performed using the pressure drop data from experiments [9]. Total of 13 experiments reported in [9] for the particle diameters 3 and 6 mm at pressures of 1 and 3 bars and inflow velocities up to 7.2 mm/s were taken. For each experiment, the variance V was calculated (see Eq. (16)), after which the sum of all the variances (unweighted) was used as the response function for optimization under DAKOTA. In the first optimization run, five model parameters listed in Table 1 were varied, except the fixed nL = nG = 3. In the second run, seven model parameters (including nL and nG) were varied.

In Fig. 5, the standard deviations σ are plotted for each experiment (parameters are listed to the right of the graph) obtained for the original Schulenberg and Müller's model [5] and its optimized versions. It should be noted that the initial standard deviation of experiment 1 is much higher than those of other experiments, and during the optimization, mainly this quantity was reduced at the expense of increase in other standard deviations. Therefore, experiment 1 was excluded from the optimization data set (i.e., optimization was carried out over the remaining 12 experiments), but its standard deviations are plotted in Fig. 5.

The parameters obtained by model optimization are presented in Table 2, together with the original parameters of models [2-5]. For the 7-parameter optimized SMO model, noticeable are the increase in the permeability exponents from 3 to about 4.5, and decrease in the drag force constants. To see the effect of model parameter adjustment, the pressure drops are plotted in Fig. 6 for several experiments [9] and corresponding calculations.

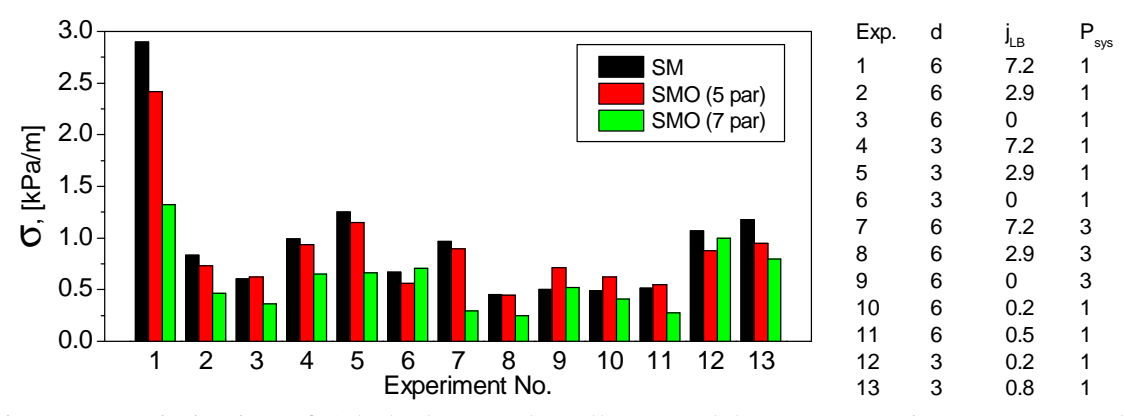


Figure 5 Optimization of Schulenberg and Müller's model [5] on experiments [9]: standard deviations for each experiment are shown for the original model (SM), and optimized model (SMO) with 5 and 7 variable parameters.

| Model | nL | nG | mL | mG | mGL | mGH | C_{SM} | nSM |
|-------------------------------|------|------|------|------|-----|------|----------|------|
| Lipinski [2] | 3 | 3 | 3 | 3 | - | - | - | - |
| Reed [3] (R) | 3 | 3 | 5 | 5 | - | - | - | - |
| Hu & Theofanous [4] | 3 | 3 | 6 | 6 | - | - | - | - |
| Optimized "classic" (CO) | 3 | 3 | 4.53 | 4.53 | - | - | - | - |
| Schulenberg & Müller [5] (SM) | 3 | 3 | 5 | - | 4 | 6 | 350 | 7 |
| SMO, 5-parameter optimized | 3 | 3 | 4.84 | - | 4 | 5.96 | 294 | 7.28 |
| SMO, 7-parameter optimized | 4.52 | 4.46 | 4.53 | - | 4 | 4.94 | 118 | 6.40 |

Table 2 Parameters of original and optimized models.

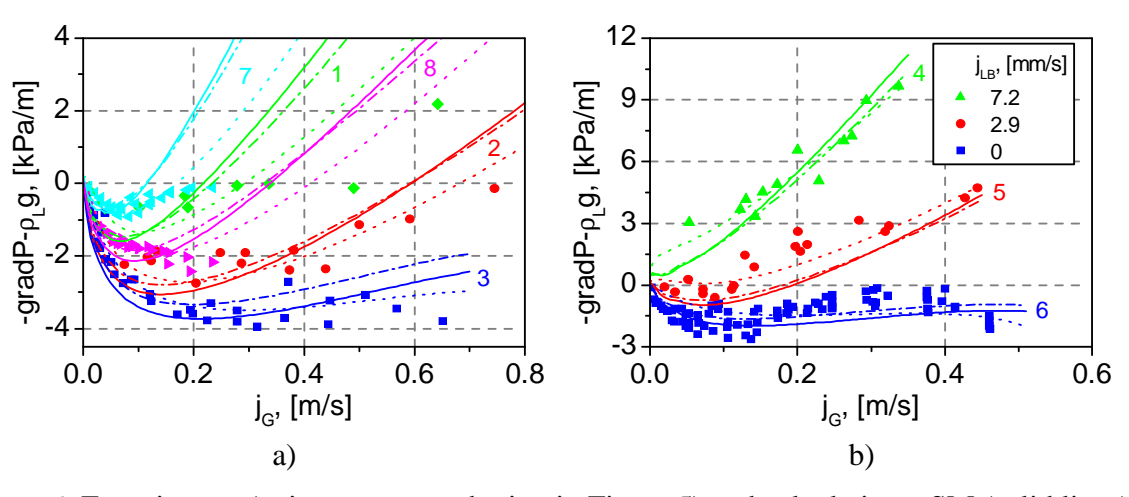


Figure 6 Experiments (points – see numbering in Figure 5) and calculations: SM (solid lines), SMO-5 parameter optimization (dash-dot lines), SMO-7 parameter optimization (dotted lines): a) 6 mm particles, b) 3mm particles.

While the above optimization improved the agreement with experimental data on pressure drop, it is important to see what effect it had on the DHF prediction. The dependencies of DHF on the particle diameters ($\varepsilon = 0.4$, $P_{sys} = 1$ bar) calculated with the optimized parameters are plotted in Fig. 4a. In the legend, the root mean square deviations $\sigma = V^{1/2}$ are given. Evidently, the parameter set obtained in 7-parameter optimizations gives underestimated DHFs due to the increased porous drag of phases caused by increased relative permeability exponents. The 5-parameter optimization, however, gives better agreement than the original SM model, however, the deviation is still larger than for Reed's and optimized classic models.

6. Uncertainty study for DHF

Consider now the uncertainties in the DHF caused by the uncertainties of the physical parameters $(d, \varepsilon, P_{sys})$. The cumulative distribution functions (CDF) for the dryout heat flux obtained by the Monte Carlo sampling of the three physical parameters in the ranges listed in Table 1 are presented in Fig. 7a for the inflow velocities $j_{LB} = 0$, 0.5 and 1 mm/s. For each input variable, uniform probability density was assumed because the data available are too scarce for a more specific choice (e.g., the distribution function for d should reflect the probability that a debris bed with that particular mean particle diameter would be formed in different accident scenarios of melt release; therefore, the distribution functions for particle diameters formed in a experiments, e.g., those from [12], cannot be used for this purpose). To assess the influence of model parameters (epistemic uncertainty), calculations were carried out for four models: Reed's model (R), optimized classic model (CO), original Schulenberg and Müller's model (SM) and its version obtained by 5-parameter optimization on the pressure drop experiments (SMO). In Fig. 7b, the probability density functions (PDF) obtained for the CO model by differentiating the corresponding CDFs are shown for $j_{LB} = 0$, 0.5, and 1 mm/s. One can see that in the case of bottom-fed debris bed, PDF becomes very asymmetric, because its left "wing" corresponds to the smaller particles, lower porosities and system pressures for which, as was shown in section 4.2.1 (see Fig. 2d) DHF becomes insensitive to debris bed parameters and approaches to its asymptotic value.

In Table 3, the values of DHF corresponding to 5% CDF are listed for different models and inflow velocities (these can be regarded "safe" levels which will not be exceeded with 95% probability, given the ranges of physical parameters assumed in Table 1). Importantly, the discrepancy between predictions of different drag model are small for this quantity (within 6% for top-fed debris bed and within 0.5% for bottom-fed).

For better understanding of the effect of uncertainties in the physical parameters, it is necessary to determine what fraction of DHF variance is attributed to each of them. The Sobol variance decomposition [17, 19, 20] was performed using the tools available in DAKOTA: the variance of DHF is decomposed into linear, quadratic and higher-order terms: $V = \sum V_i + \sum V_{ij} + \dots$, where V_i are linear effects of each uncertain parameter, V_{ij} are effects of interactions between i-th and j-th parameters etc. Of interest are the total sensitivity indices $S_{Ti} = (V_i + V_{ij} + \dots)/V$, where the sum contains all terms corresponding to i-th parameter. S_{Ti} shows by what fraction the variance of DHF will be reduced if the i-th parameter is fixed

(its uncertainty is eliminated). Note that the sum of Sobol total sensitivity indices is greater than unity because higher-order terms are counted several times, the sum would be unity only in the case of purely additive, i.e., non-interacting, inputs.

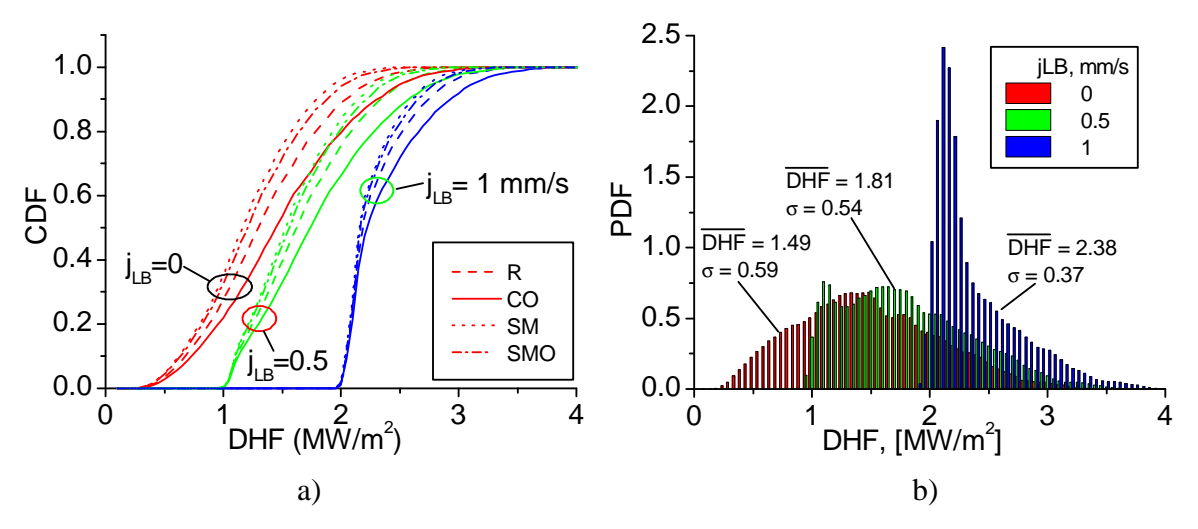
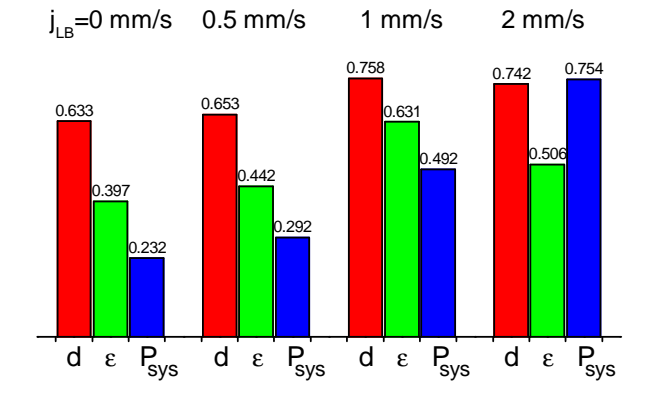


Figure 7 Distribution functions for DHF due to uncertainties in physical parameters: a) cumulative distribution functions for different drag models, b) probability density functions for optimized "classic" model (mean values and standard deviations are in MW/m^2).

In Fig. 8 the Sobol total sensitivity indices are presented for the top-fed and bottom-fed debris beds (model CO). One can see that about 63-76% of the DHF variance is due to the uncertainty in particle diameter, 40-63% due to porosity. System pressure uncertainty gives 23-49% input into DHF variance for inflow velocities up to 1 mm/s, while for $j_{LB} = 2$ mm/s the input of system pressure increases to 75%. This confirms the results of Morris sensitivity analysis presented in Fig. 2c where it was shown that system the influence of system pressure on DHF increases with the inflow velocity. However, it should be noted that sensitivity indexes for different input uncertain parameters might change if ranges of these parameters or their distributions will be selected in a different way.



| Figure 8 | Sobol total sensitivity indices | S_{Ti} |
|----------|---------------------------------|----------|
| for DHF | | |

| Model | $j_{LB}=0$ | 0.5 | 1.0 |
|----------|------------|--------|--------|
| R | 0.547 | 1.070 | 2.023 |
| CO | 0.583 | 1.073 | 2.028 |
| SM | 0.508 | 1.064 | 2.017 |
| SMO | 0.515 | 1.065 | 2.023 |
| Mean/ | 0.539/ | 1.068/ | 2.023/ |
| σ | 0.034 | 0.004 | 0.005 |

Table 3 DHF (MW/m^2) at CDF = 5%

7. Conclusions

Sensitivity analysis and optimization of model parameters allow one to obtain better agreement between the predictions and experiments. However, "blind" optimization of all model parameters with respect to a chosen set of data can deteriorate predictions of other quantities, as was demonstrated by optimization of drag models on the pressure drop experiments which resulted in worse prediction of DHF. For the chosen debris bed parameters, it was shown that the model-to-model differences are noticeable on the cumulative distribution functions. However, the lower "safe" boundary, corresponding to 5% of cumulative distribution function of DHF, is predicted by all models in quite narrow range. It will be important to assess the modeling uncertainties in evaluation of the coolability margins for 2D and 3D configurations of the debris beds.

8. Acknowledgements

The work is supported by the Swedish Nuclear Radiation Protection Authority (SSM), Swedish Power Companies, European Commission (SARNET-2), Nordic Nuclear Safety Program (NKS), Swiss Federal Nuclear Safety Inspectorate (ENSI) under the APRI-MSWI program at the Royal Institute of Technology (KTH), Stockholm, Sweden. Authors are grateful to Professor Truc-Nam Dinh from Idaho National Lab, USA for very useful comments and discussions.

9. References

- [1] M. Bürger, M. Buck, G. Pohlner, S. Rahman, R. Kulenovic, F. Fichot, W. Ma, J. Miettinen, I. Lindholm and K. Atkhen, "Coolability of particulate beds in severe accidents: Status and remaining uncertainties," *Progress in Nuclear Energy*, Vol. 52, 2010, pp. 61-75.
- [2] R. Lipinski, "A one dimensional particle bed dryout model," *ANS Trans.*, Vol. 38, 1981, pp. 386-387.
- [3] A. Reed, "The effect of channeling on the dryout of heated particulate beds immersed in a liquid pool," PhD thesis, MIT, Cambridge, 1982.
- [4] K. Hu and T. Theofanous, "On the measurement and mechanism of dryout in volumetrically heated coarse particle beds," *Int. J. Multiphase Flow*, Vol. 17, No. 4, 1991, pp. 519-532.
- [5] T. Schulenberg and U. Müller, "An improved model for two-phase flow through beds of course particles," *Int. J. Multiphase Flow*, Vol. 13, No. 1, 1987, pp. 87–97.
- [6] V. X. Tung and V. K. Dhir, "A hydrodynamic model for two-phase flow through porous media," *Int. J. Multiphase Flow*, Vol. 14, No. 1, 1988, pp. 47–65.
- [7] W. Schmidt, "Interfacial drag of two-phase flow in porous media," *Int. J. Multiphase Flow*, Vol. 33, 2007, pp. 638-657.

- [8] I. Lindholm, S. Holmström, J. Miettinen, V. Lestinen, J. Hyvärinen, P. Pankakoski, H. Sjövall, "Dryout heat flux experiments with deep heterogeneous particle bed," *Nucl. Eng. Design*, Vol. 236, 2006, pp. 2060-2074.
- [9] P. Schäfer, M. Groll, R. Kulenovic, "Basic investigations on debris bed cooling," *Nucl. Eng. Design*, Vol. 236, 2006, pp. 2104-2116.
- [10] P.P. Kulkarni, M. Rashid, R. Kulenovic and A.K. Nayak, "Experimental investigation of coolability behaviour of irregularly shaped particulate debris bed," *Nucl. Eng. Design*, Vol. 240, 2010, pp. 3067-3077.
- [11] S. Ergün, "Fluid flow through packed columns," *Chem. Eng. Prog.*, Vol. 48, 1952, pp. 89-94.
- [12] P. Kudinov, A. Karabojan, W. Ma and T.-N. Dinh, "The DEFOR-S experimental study of debris formation with corium simulant materials," *Nuclear Technology*, Vol. 170, 2010, pp. 219-230.
- [13] P. Kudinov, V. Kudinova, and T.-N. Dinh, "Molten Oxidic Particle Fracture during Quenching in Water," 7th International Conference on Multiphase Flow ICMF 2010, Tampa, FL USA, May 30-June 4, 2010.
- [14] P. Kudinov, A. Karbojian, C.-T. Tran, W. Villanueva, "The DEFOR-A Experiment on Fraction of Agglomerated Debris as a Function of Water Pool Depth," The 8th International Topical Meeting on Nuclear Thermal-Hydraulics, Operation and Safety (NUTHOS-8), Shanghai, China, October 10-14, N8P0296, 2010.
- [15] D. Magallon, "Characteristics of corium debris bed generated in large-scale fuel-coolant interaction experiments," *Nucl. Eng. Design*, Vol. 236, 2006, pp. 1998-2009.
- [16] P. Kudinov and T.-N. Dinh, "An analytical study of mechanisms that govern debris packing in a LWR severe accident", The 12th International Topical Meeting on Nuclear Reactor Thermal Hydraulics (NURETH-12), Sheraton Station Square, Pittsburgh, Pennsylvania, U.S.A. September 30-October 4, 2007. Paper 247.
- [17] DAKOTA, A Multilevel Parallel Object-Oriented Framework for Design Optimization, Parameter Estimation, Uncertainty Quantification, and Sensitivity Analysis. Version 5.0 User's Manual. Sandia National Laboratories, 2010.
- [18] M. D. Morris, "Factorial sampling plans for preliminary computational experiments," *Technometrics*, Vol. 33, No. 2, 1991, pp. 161–174.
- [19] A. Saltelli, S. Tarantola, F. Campolongo, M. Ratto, Sensitivity Analysis in Practice. John Wiley & Sons, Ltd, 2004, 232 p.
- [20] I. M. Sobol, "Sensitivity analysis for non-linear mathematical models," *Math. Modelling & Comp. Exp.*, Vol. 1, 1993, pp. 407–414.